

## Accepted Manuscript

Discovery of potent aryl-substituted 3-[(3-methylpyridine-2-carbonyl) amino]-2,4-dimethyl-benzoic acid EP4 antagonists with improved pharmacokinetic profile

Maria-Jesus Blanco, Tatiana Vetman, Srinivasan Chandrasekhar, Matthew J. Fisher, Anita Harvey, Mark Chambers, Chaohua Lin, Daniel Mudra, Jennifer Oskins, Xu-Shan Wang, Xiao-Peng Yu, Alan M. Warshawsky

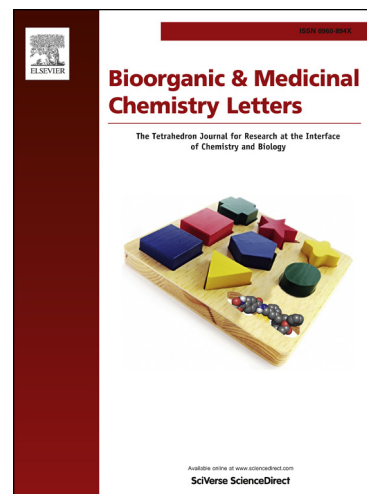
PII: S0960-894X(15)30370-X  
DOI: <http://dx.doi.org/10.1016/j.bmcl.2015.12.057>  
Reference: BMCL 23418

To appear in: *Bioorganic & Medicinal Chemistry Letters*

Received Date: 16 November 2015  
Revised Date: 16 December 2015  
Accepted Date: 17 December 2015

Please cite this article as: Blanco, M-J., Vetman, T., Chandrasekhar, S., Fisher, M.J., Harvey, A., Chambers, M., Lin, C., Mudra, D., Oskins, J., Wang, X-S., Yu, X-P., Warshawsky, A.M., Discovery of potent aryl-substituted 3-[(3-methylpyridine-2-carbonyl) amino]-2,4-dimethyl-benzoic acid EP4 antagonists with improved pharmacokinetic profile, *Bioorganic & Medicinal Chemistry Letters* (2015), doi: <http://dx.doi.org/10.1016/j.bmcl.2015.12.057>

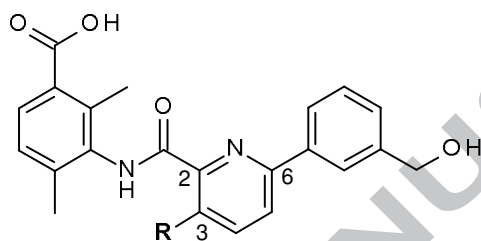
This is a PDF file of an unedited manuscript that has been accepted for publication. As a service to our customers we are providing this early version of the manuscript. The manuscript will undergo copyediting, typesetting, and review of the resulting proof before it is published in its final form. Please note that during the production process errors may be discovered which could affect the content, and all legal disclaimers that apply to the journal pertain.



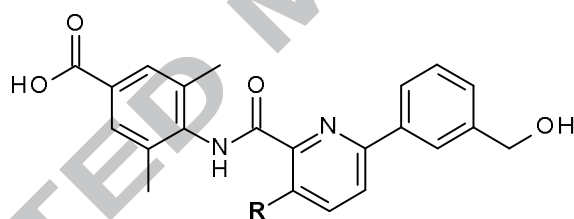
## Graphical Abstract

Discovery of potent aryl-substituted 3-[(3-methylpyridine-2-carbonyl) amino]-2,4-dimethyl-benzoic acid EP4 antagonists with improved pharmacokinetic profile

Maria-Jesus Blanco,\* Tatiana Vetman, Srinivasan Chandrasekhar, Matthew J. Fisher, Anita Harvey, Mark Chambers, Chaohua Lin, Daniel Mudra, Jennifer Oskins, Xu-Shan Wang, Xiao-Peng Yu, and Alan M. Warshawsky



7a-b



8a-b

# Discovery of potent aryl-substituted 3-[(3-methylpyridine-2-carbonyl) amino]-2,4-dimethyl-benzoic acid EP4 antagonists with improved pharmacokinetic profile

Maria-Jesus Blanco,\* Tatiana Vetman, Srinivasan Chandrasekhar, Matthew J. Fisher, Anita Harvey, Mark Chambers, Chaohua Lin, Daniel Mudra, Jennifer Oskins, Xu-Shan Wang, Xiao-Peng Yu, and Alan M. Warshawsky

Lilly Research Laboratories, Eli Lilly and Company, Indianapolis, IN 46285

**Abstract:** Two new series of EP4 antagonists containing a 3-methylaryl-2-carbonyl core have been identified. One series has a 3-substituted-phenyl core, while the other one incorporates a 3-substituted pyridine. Both series led to compounds with potent activity in functional and human whole blood (hWB) assays. In the pyridine series, compound **7a** was found to be a highly potent and selective EP4 antagonist, with suitable rat and dog pharmacokinetic profiles.

Keywords: EP4 receptor antagonist; structure-activity relationship (SAR); Prostaglandin E2; human whole blood (hWB) assay; inflammation; pain

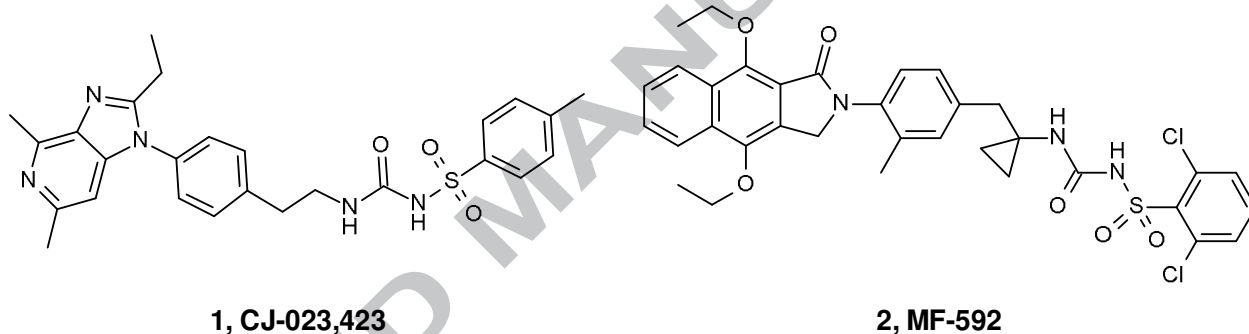
Prostaglandin E2 (PGE2)<sup>1</sup> is an endogenous lipid belonging to the prostaglandin superfamily. Prostaglandins, including thromboxanes and prostacyclins, are enzymatically derived from fatty acids and have a variety of robust physiological effects in the human body. PGE2, an important pro-inflammatory messenger, is formed by metabolism of arachidonic acid and elicits its biological functions through four EP subtype receptors EP1-4, all belonging to the G-protein-coupled receptor (GPCR) superfamily. There are several pathological conditions wherein PGE2 plays a major role, making EP receptors an appropriate pharmacological target. Because PGE2 predominantly serves as a signaling molecule in inflammation, most approaches to modulate EP receptors have focused on inflammatory conditions, although EP receptor modulators might also be beneficial in the treatment of other disorders like oncology<sup>2</sup> and treatment of functional bladder disorders.<sup>3</sup> The identification of highly selective EP1, EP3 and EP4 antagonists, has led to pharmacological demonstration that EP4, not EP1 or EP3, is the primary receptor involved in joint inflammation and pain in rodent models of rheumatoid and osteoarthritis. Since EP4 does not interfere directly with the biosynthesis of any of the prostanoids, a selective EP4 antagonist might provide analgesia without the potential side effects observed with NSAIDs and COX-2 inhibitors.<sup>4, 5</sup>

---

\* Corresponding author. Tel.: +1-317-433-3612; e-mail: blanco\_maria@lilly.com

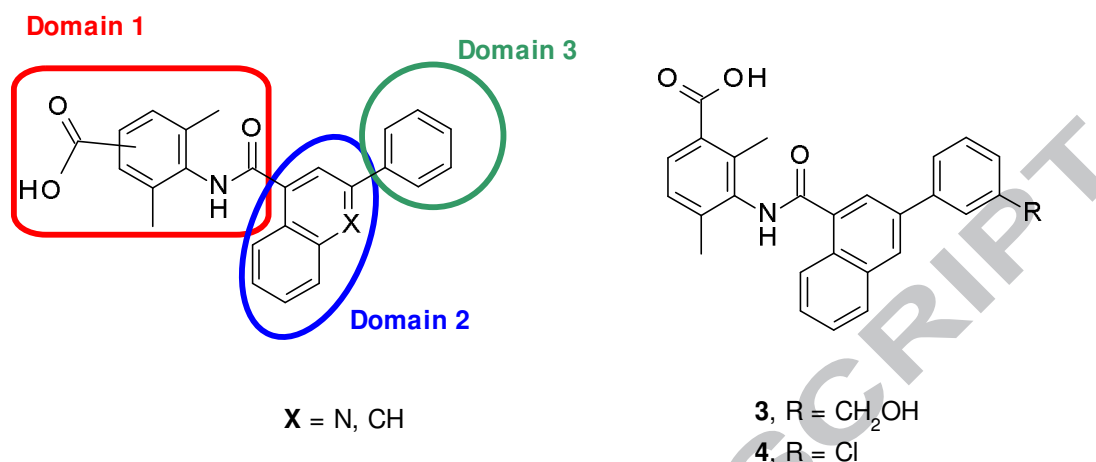
Growing interest from the pharmaceutical industry for developing safer analgesics makes EP4 antagonism an attractive target and has led to the discovery of several advanced compounds in the past few years. CJ-023,423 (**1**, Figure 1) was the first EP4 antagonist evaluated in the clinic for the treatment of signs and symptoms of osteoarthritis (OA). This compound achieved a positive proof-of-concept in chronic inflammatory pain (OA pain) in a phase II study in 2007.<sup>6</sup> More recently, Merck-Frosst reported the discovery of a series of naphthalene and quinoline amides and sulfonylureas that culminated in the discovery of MF-592<sup>7</sup> (**2**, Figure 1). MF-592 demonstrated good functional potency (hEP4 IC<sub>50</sub> = 3 nM) and potent inhibition of PGE2 modulated TNF $\alpha$  release in LPS stimulated human whole blood (hWB) (IC<sub>50</sub> = 78 nM). In addition, it showed an excellent oral pharmacokinetic (PK) profile and in vivo efficacy in a rat chronic adjuvant-induced-arthritis model (ED<sub>50</sub> = 0.1 mg/kg/day).

Figure 1. Examples of advanced EP4 antagonists. Clinical candidate CJ-023,423 (**1**) and MF-592 (**2**).



We have previously reported the discovery of novel quinoline and naphthalene analogs with potent EP4 antagonist activity.<sup>8</sup> From this series compound **3**, (Figure 2) showed excellent hWB activity (IC<sub>50</sub> = 6 nM) but suffered from a poor oral PK profile (rat %F = 6). In contrast, compound **4** (Figure 2), displayed modest hWB activity (IC<sub>50</sub> = 243 nM) but excellent oral rat bioavailability (100%). During the course of our research, we explored replacements for the central domain of the molecules, to identify compounds with high ligand efficiencies<sup>9</sup> (LEAN values),<sup>8</sup> potent hWB activities and acceptable ADME profiles.

Figure 2. Previously reported EP4 antagonists series



Toward this goal, we synthesized several substituted phenyl- and pyridine-containing analogs of compounds **3** and **4**. Replacement of the naphthalene core of **3** with a 2-methyl-benzene core gave **5a**, which maintained the same level of functional activity (hEP4 IC<sub>50</sub> = 2.31 nM) as its bicyclic analog (Figure 3, Table 1). Compound **5a** also showed potent hWB activity (IC<sub>50</sub> = 59.5 nM). Introduction of a 2-fluoro-benzene core led to **5b** with activity comparable to the 2-Me analog, (hEP4 IC<sub>50</sub> = 4.49 nM and hWB IC<sub>50</sub> 72.4 nM). Para-2,5-dimethyl-benzoic acid derivatives, **6a** (R=Me) and **6b** (R=F) showed sub-nanomolar functional activity (0.28 and 0.78 nM, respectively) with hWB IC<sub>50</sub> values < 50 nM. While the functional activity is not corrected for human serum protein binding, the hWB assay is a native tissue assay that represents relevant physiological conditions.<sup>10</sup> Therefore, the hWB assay was important for choosing molecules to evaluate further.

Replacement of the naphthalene with a 3-methyl-pyridine core gave **7a**, with high potencies in the functional (hEP4 IC<sub>50</sub> = 2.36 nM) and hWB (IC<sub>50</sub> <40 nM) assays. Introduction of a trifluoromethyl substituent offered the possibility to modulate electronic and steric effects on the central ring,<sup>11</sup> noting that the molecular volume of CF<sub>3</sub> resembles an isopropyl group. Trifluoromethyl analog **7b**, demonstrated activities equivalent to methyl analog **7a**, (**7b**, hEP4 IC<sub>50</sub>= 1.94 nM) with hWB IC<sub>50</sub> = 59 nM.

The para-2,5-dimethyl-benzoic acid derivatives (**8a** and **8b**) showed sub-nanomolar functional activity (~3-fold improvement over **7a**, **7b**) that failed to translate to increases in hWB activity (IC<sub>50</sub> >50 nM).

Compound **9** combined the 3-methyl-pyridine central core with the 3-chloro-benzene substitution in domain 3 as in compound **4**. However, the potent functional activity (hEP4 IC<sub>50</sub>=1.56 nM) for compound **9** did not translate to potent activity (>600 nM) in the hWB assay.

Overall, the modifications to the central core (domain 2) were favorable. Most of the compounds showed potent hWB activity, more than 10-fold more potent than clinical candidate CJ-023,423 (hWB IC<sub>50</sub> = 1600 nM).<sup>8</sup>

With respect to physicochemical properties and ligand efficiency, compounds **5-9** had MW <450, cLogD<3, and the LEAN values were maintained or increased (0.27-0.33) relative to quinoline/naphthalene analogs. Those attributes were targeted for potential improvements in pharmacokinetic profiles.

Figure 3. Structures of **5-9** compounds

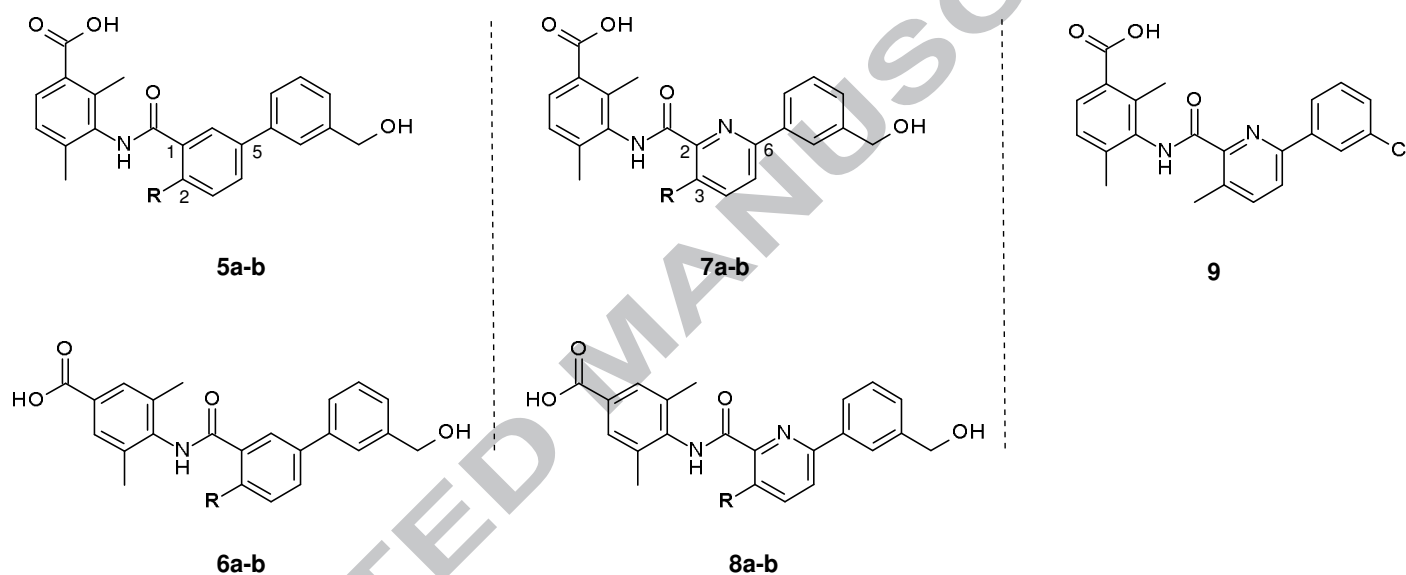


Table 1. *In vitro* functional activity and human whole blood (hWB) data of key analogs.

Compd	R	MW	hEP4 functional cAMP IC <sub>50</sub> (nM) <sup>a</sup>	hWB IC <sub>50</sub> (nM) <sup>a</sup>	LEAN <sup>b</sup> values	cLog D <sup>c</sup>
<b>3</b>	-	426	2.42 + 1.1 (5)	6.2 + 4.5 (3)	0.28	2.48
<b>4</b>	-	430	3.62 + 0.7 (3)	243.0 + 116 (6)	0.27	3.85
<b>5a</b>	-Me	389	2.31 ± 2.02 (2)	59.5 ± 37.8 (3)	0.30	2.00
<b>5b</b>	-F	393	4.49 ± 1.90 (4)	72.4 ± 58.2 (16)	0.29	1.63
<b>6a</b>	-Me	389	0.28 ± 0.13 (5)	18.7 ± 13.6 (6)	0.33	2.08
<b>6b</b>	-F	393	0.73 ± 0.48 (6)	47.8 ± 15.2 (5)	0.32	1.71
<b>7a</b>	-Me	390	2.36 ± 1.42 (5)	38.7 ± 17.1 (9)	0.30	1.55
<b>7b</b>	-CF <sub>3</sub>	444	1.94 ± 0.93 (4)	59.0 ± 39 (3)	0.27	1.92

<b>8a</b>	-Me	390	0.67 ± 0.24 (3)	56.3 ± 34.3 (10)	0.32	1.64
<b>8b</b>	-CF <sub>3</sub>	444	0.67 ± 1.55 (3)	121.0 ± 58 (5)	0.29	2.00
<b>9</b>	-Me	395	1.56 ± 0.75 (2)	637 ± 298 (3)	0.32	2.93

- Results are expressed as the geometric mean ± standard deviation; n = number of independent determinations. The standard deviation is calculated by the delta method, being SDlogIC<sub>50</sub> x geometric mean x ln(10). For additional details on the assays please see ref 10.
- LEAN values are based on functional activity and defined as -log(IC<sub>50</sub>)/number of non-hydrogen atoms.
- cLog D at pH=7.4, calculated using Marvin and calculator plugin freeware (www.chemaxon.com, ChemAxon Kft, Budapest, Hungary).

Data to assess solubility and rat pharmacokinetic profiles of key analogs is presented in Table 2.

Table 2. ADME/PK assessment of key analogs

Compd	R	HTSA solubility <sup>a</sup> (mg/mL)	Rat iv clearance <sup>b</sup> (mL/min/kg)	po AUC <sup>c</sup> (ng*h/mL)	% F <sup>b,c</sup> , rat
<b>5a</b>	-Me	0.783	15	375	7
<b>5b</b>	-F	0.709	30	994	11-54*
<b>6a</b>	-Me	0.031	71	88	13
<b>6b</b>	-F	0.774	91	105	12
<b>7a</b>	-Me	0.242	2.2	8520	22
<b>7b</b>	-CF <sub>3</sub>	0.029	7.0	1540	13
<b>8a</b>	-Me	0.014	7.0	4330	36
<b>8b</b>	-CF <sub>3</sub>	0.023	54	243	16

- High Throughput Solubility Assay (HTSA), assessment of aqueous solubility at pH=6. Samples prepared in DMSO were dried for 12 hours. The powder or film was re-dissolved in the solvent at pH 6 and DMSO control at 2mM target concentration. Samples are stirred for 20 hours and filtered through a 0.7 μm GF filter. The filtrate was analyzed by HPLC assay for concentration against DMSO standard curve.
  - Dose of 1 mg/kg iv.
  - Dose of 5 mg/kg po.
- \*Significant variability observed

We noted that small changes in the molecular structure had significant and unpredictable effects on solubility, clearance and plasma exposure. The compounds with a phenyl moiety in domain 2 (**5a**, **5b**, **6a**, **6b**), showed good solubility in general, although they suffered from poor oral bioavailability and high clearance. The analogs with a pyridine group in domain 2 (**7a**, **7b**, **8a**, **8b**) tended to have low solubility (except

**7a**), but showed lower clearance (except **8b**) and acceptable oral bioavailability. Based on the combination of solubility and rat PK profile, compound **7a** was selected for further characterization.

Compound **7a** showed an acceptable pharmacokinetic profile in a dog study with increased oral bioavailability (48%).

Table 3. Pharmacokinetic profiling for compound **7a**<sup>6</sup>

Species	iv/po dose (mg/kg)	po AUC (ng*h/mL)	po Cmax (ng/mL)	po T1/2 (h)	iv CL (mL/min/kg)	Vdss (L/Kg)	F (%)
rat	1/5	8520	1640	2.1	2.2	0.16	22
dog	1/5	10900	3820	1.1	3.7	0.97	48

Compound **7a** was tested in binding assays to assess selectivity against the other EP receptor subtypes (Table 3). No detectable binding was observed with either EP1, EP2, or EP3. In addition, compound **7a** was found to have no *in vitro* inhibitory activity against several CYP enzymes up to 10  $\mu$ M. Therefore the risk of drug-drug interactions with **7a** was expected to be low. Furthermore, **7a** was evaluated at Cerep for broader selectivity against a panel of 13 receptors, four ion channels, one transporter, and one enzyme. No significant activity on any of the targets at 10  $\mu$ M was noted.<sup>12</sup> Finally, **7a** had no activity up to 100  $\mu$ M against hERG in a [<sup>3</sup>H]-astemizole binding assay.

Table 3. Selectivity data for **7a**.

Assay	Results <sup>a</sup>
hEP <sub>1</sub> binding	$K_i > 17.5 \mu\text{M}$ ; $\text{IC}_{50} > 25 \mu\text{M}$ (2)
hEP <sub>2</sub> binding	$K_i > 18.9 \mu\text{M}$ ; $\text{IC}_{50} > 25 \mu\text{M}$ (5)
hEP <sub>3</sub> binding	$K_i > 14 \mu\text{M}$ ; $\text{IC}_{50} > 25 \mu\text{M}$ (5)
CYP1A2, CYP2B6, CYP2C19, CYP2C8, CYP2C9, CYP2D6, CYP3A4 inhibition	$\text{IC}_{50} > 10 \mu\text{M}$ for all

<sup>a</sup>Expressed as geometric mean  $\pm$  geometric standard deviation, with number of replicates in parentheses.

To establish pain relief efficacy in rats, compound **7a** was tested in the monoiodoacetic acid (MIA) model of joint pain. Functional *in vitro* activity showed no

significant differences between human and rat EP4 for compound **7a**. The injection of MIA into the knee joint of rats produces an acute inflammatory insult which develops into chronic degeneration of the tissues in the injected joint and pain. This pain can be measured via differential weight bearing of the hind legs using an incapacitance tester.<sup>13</sup> Efficacy is assessed as by the ability of a test compound to normalize weight distribution indicating reduction of joint pain. The MIA model has been extensively described in the literature<sup>14</sup> and has been used to demonstrate pain reversal for a variety of mechanisms with compounds showing efficacy at plasma exposures comparable to clinically effective human exposures.<sup>15</sup>

Figure 4 showed the results for the experiment where rats were injected intra-articularly with 0.3 mg MIA in 50  $\mu$ l saline into the right knee with 50  $\mu$ l saline injected into the left knee on day 0. Twelve days later, the rats were randomized and dosed orally with either vehicle, 0.3, 1, 3 or 10 mg/kg compound **7a**, or the positive control non-steroidal anti-inflammatory drug (NSAID) diclofenac at 5 mg/kg. Efficacy was measured using incapacitance testing 30 minutes post dose. Compound **7a** dose dependently inhibited differential weight bearing versus vehicle at 3 and 10 mg/kg as did the NSAID diclofenac.

As compound **7a** inhibits PGE2 actions at the EP4 receptor it would also be expected to inhibit inflammation. For assessing efficacy versus inflammation the rat adjuvant induced arthritis (AIA) model was used. This model has been well-described in the literature<sup>16</sup> and has been used to demonstrate efficacy versus inflammation for a variety of mechanisms and compounds including those that target prostaglandin pathways such as NSAIDs. Efficacy is measured as the ability of a test compound to inhibit paw swelling.

Figure 5 showed the results for the experiment where rats had their paw widths measured and were then inoculated with 0.25 mg of adjuvant (M. Tuberculosis H37 RA) in 100  $\mu$ l of mineral oil intradermal at the base of the tail to induce adjuvant disease (day 0). Eleven days post inoculation paw width of both right and left paws was measured again and the percent change from the day 0 reading calculated. This measurement along with the body weight of the rats was used to randomize the animals and the rats were dosed with vehicle and compound **7a** at doses of 1, 3 and 10 mg/kg. The nonsteroidal anti-inflammatory drug (NSAID) diclofenac was included at a dose of 10 mg/kg as a positive control. On day 15 post adjuvant injection the rats were euthanized without further dosing and paw width measured again. The percent increase in mean paw thickness from day 11 to day 15 was then calculated as a measure of paw swelling which is indicative of the amount of inflammation in the paws. Compound **7a** significantly inhibited increases in paw inflammation (swelling) compared to vehicle at doses of 10 and 30 mg/kg as did the NSAID diclofenac.

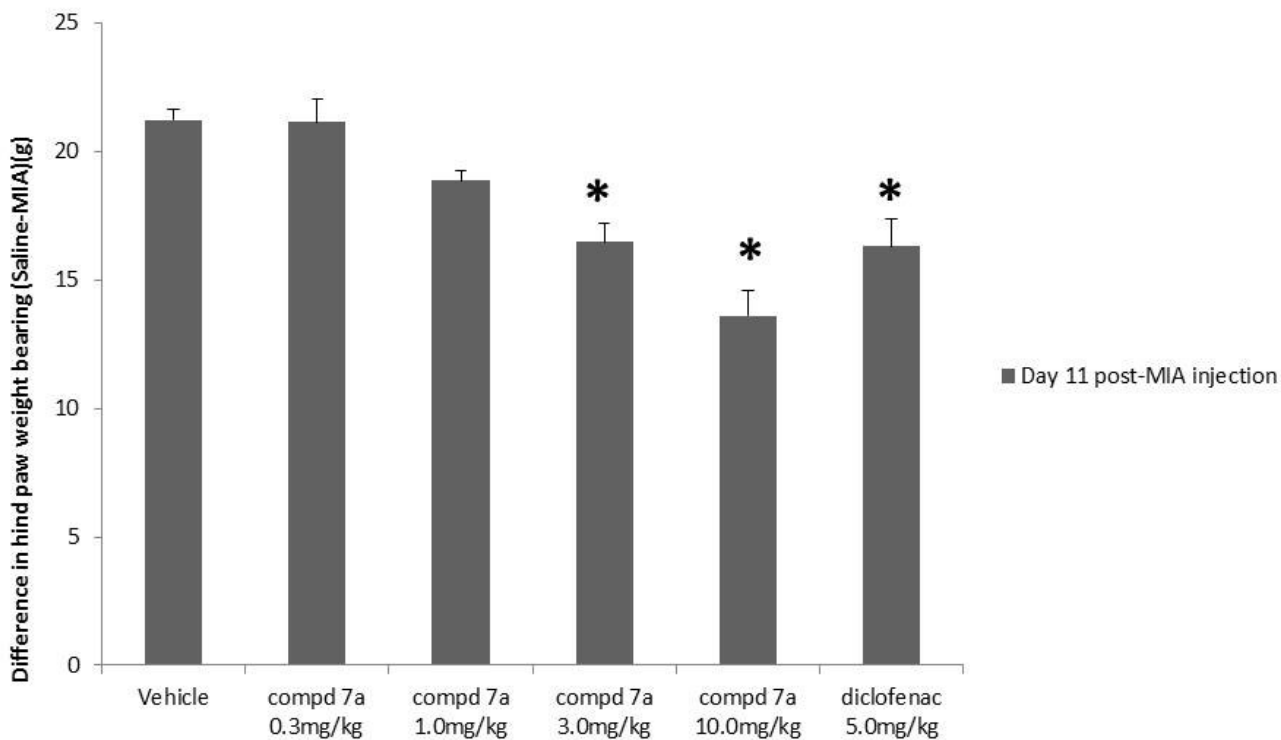


Figure 4: Dose response study with compound 7a in the MIA model with pain measured one hour post dose. The data are presented as mean  $\pm$  SEM where group size is  $n = 5$ . Statistical comparison to vehicle: Dunnett's test ( $*p < 0.05$ ). Vehicle is 10% Acacia in water plus 0.05% antifoam.

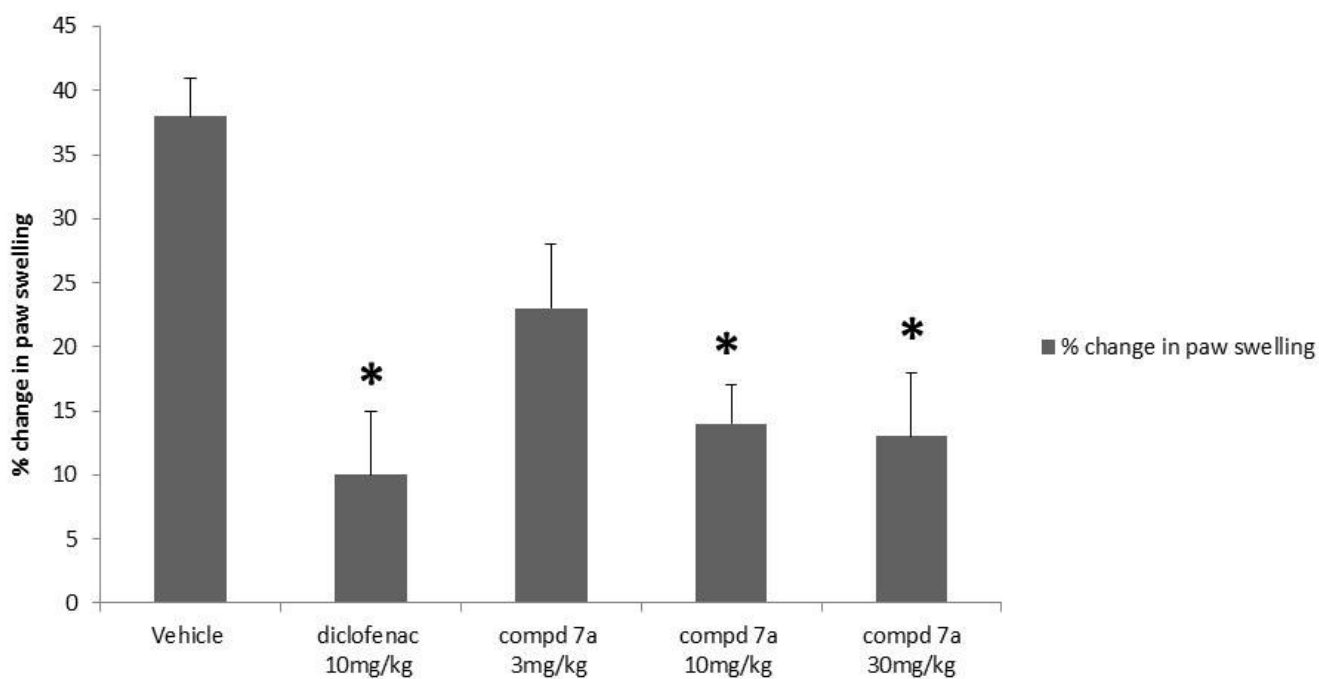
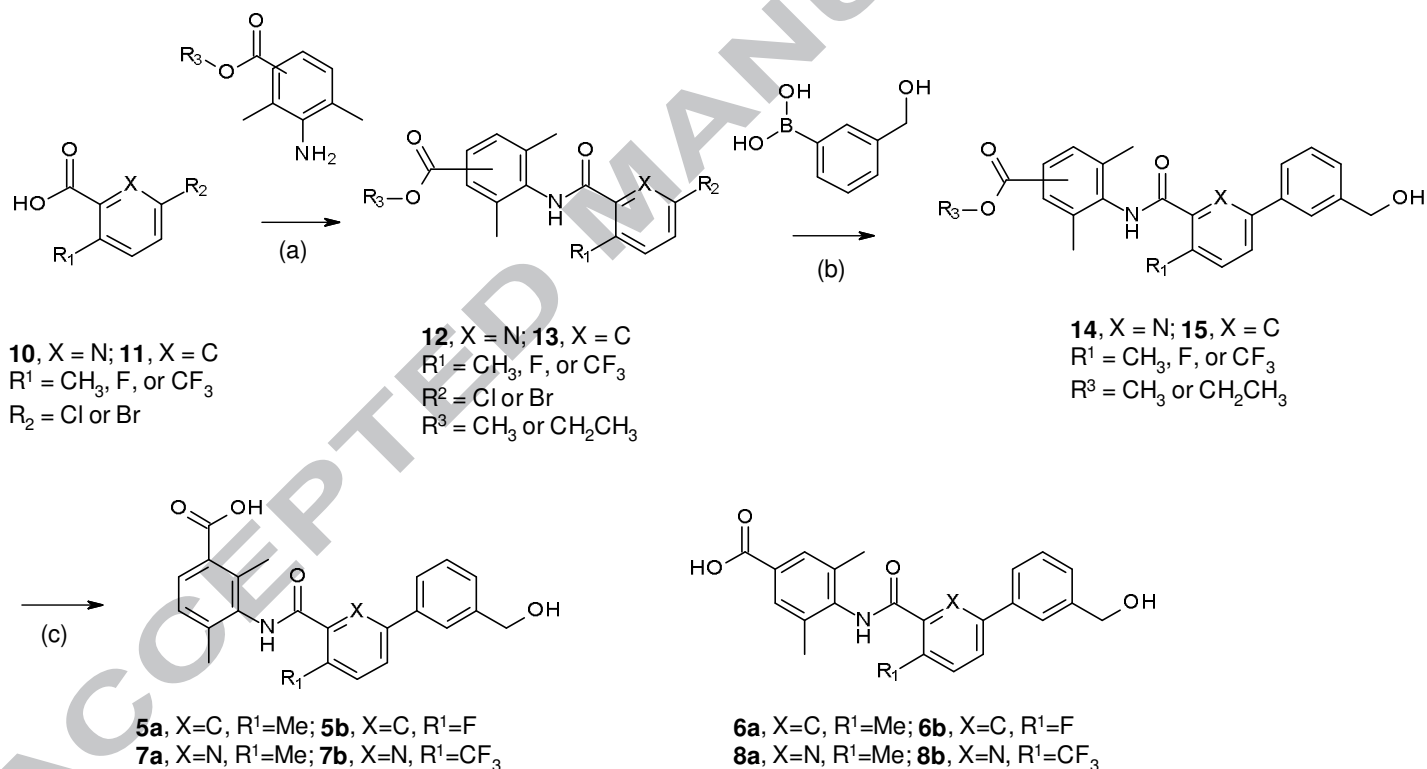


Figure 5: Dose response study with compound 7a in the AIA model to assess inhibition of increase in paw swelling. The data are presented as mean  $\pm$  SEM where group size is  $n = 8$ . Statistical comparison to vehicle: Dunnett's test ( $*p < 0.05$ ). Vehicle is 10% Acacia in water plus 0.05% antifoam.

The compounds described in Table 1 were synthesized by the sequence shown in Scheme 1.<sup>10</sup> T<sub>3</sub>P (n-propanephosphonic acid anhydride)<sup>17</sup> mediated coupling of 3-chloro substituted pyridine (**10**) or 3-bromo substituted benzene (**11**) carboxylic acids with corresponding functionalized aniline derivative led to amides **12** or **13** in good yields. Suzuki coupling of 3-(hydroxymethyl)-phenyl-boronic acid with **12** or **13** led to triaryl derivatives **14** and **15**. Subsequent ester hydrolysis under basic conditions provided the final carboxylic acids **5-8**.

Scheme 1. General synthetic route to EP4 antagonist compounds.



Reagents and conditions: (a) T<sub>3</sub>P, CH<sub>2</sub>Cl<sub>2</sub>, DIEA, room temperature, 24 h, 28-93%; (b) 1,4-dioxane, [3-(hydroxymethyl)phenyl]boronic acid, K<sub>2</sub>CO<sub>3</sub>, PdCl<sub>2</sub>(dppf) CH<sub>2</sub>Cl<sub>2</sub>, 110 °C, 3h, 39-74%; (c) 1N NaOH, 1:1 THF/MeOH, 30-97%.

In conclusion, a novel series of potent EP4 antagonists have been identified that demonstrated potent functional activity and robust target engagement in an *ex vivo*

LPS-stimulated human whole blood (hWB) assay. Furthermore, pharmacokinetic assessment identified compound **7a** with lower rat clearance and efficient oral exposures. Compound **7a** was highly selective over EP1, EP2 and EP3. *In vivo* efficacy studies showed comparable effects to NSAID diclofenac in the pain measured MIA assay and AIA assay to assess inflammation. Further optimization of compounds from this scaffold and *in vivo* pharmacology studies will be reported in due course.

## Acknowledgements

We would like to thank Jaclyn Barrett for analytical support and solubility data.

## Supplementary data

Supplementary data (CEREP panel data) associated with this manuscript can be found, in the online version, at .....

## References

1. Kawahara, K.; Hohjoh, H.; Inazumi, T.; Tsuchiya, S.; Sugimoto, Y. *Biochim Biophys Acta* **2015**, *414*, 1851.
2. (a) Misra, S.; Sharma, K. *Curr Drug Targets* **2014**, *15*, 347; (b) Okunishi, K.; DeGraaf, A.J.; Zaslona, Z.; Peters-Golden, M. *FASEB J.* **2014**, *28*, 56.
3. Rahnama'i M.S., van Kerrebroeck P.E., de Wachter S.G., van Koevinge G.A. *Nat Rev Urol.* **2012**, *9*, 283.
4. Hippisley-Cox, J.; Coupland, C. *BMJ*, **2005**, *330*, 1366.
5. Hippisley-Cox, J.; Coupland, C.; Logan, R. *BMJ*, **2005**, *331*, 1310.
6. Borriello, M.; Stasi, L.P. *Pharm Pat Anal.* **2013**, *2*, 387.
7. Burch, J.D.; Farand, J.; Colucci, J.; Sturino, C.; Ducharme, Y.; Friesen, R.W.; Levesque, J.F.; Gagne, S.; Wrona, M.; Therien, A.G.; Mathieu, M.C.; Denis, D.; Vigneault, E.; Xu, D.; Clark, P.; Rowland, S.; Han, Y. *Bioorg Med Chem Lett* **2011**, *21*, 1041.
8. (a) Blanco M. J.; Vetman T.; Chandrasekhar S.; Fisher M.J.; Harvey A.; Mudra D.; Wang X.S.; Yu X.P.; Schiffler M.A.; Warshawsky A.M. *Bioorg. Med. Chem. Lett.* **2016**, *26*, 105. (b) LEAN is a metric for ligand efficiency and is defined as  $-\log(\text{IC}_{50})/\text{number of non-hydrogen atoms}$ .
9. Ligand efficiency is a key parameter for drug discovery. Hopkins, A.L.; Keserue, G.M.; Leeson, P.D.; Rees, D.C.; Reynolds, C.H. *Nat. Rev. Drug Discovery* **2014**, *13*, 105.
10. Synthesis protocols, compound characterization, and assay protocols have been published. Blanco-Pillado, M.-J.; Manninen, P. R.; Schiffler, M. A.; Vetman, T. N.; Warshawsky, A. M.; York, J. S. WO2015094912.
11. Hagmann, W.K. *J. Med. Chem.* **2008**, *51*, 4359.
12. For more details, please see supplemental data.
13. Benschop, R.J.; Collins, E.C.; Darling, R.J.; Allan, B.W.; Leung, D.; Conner, E.M.; Nelson, J.; Gaynor, B.; Xu, J.; Wang, X.F.; Lynch, R.A.; Li, B.; McCarty, D.; Nisenbaum, E.S.; Oskins, J.L.; Lin, C.; Johnson, K.W.; Chambers, M.G. *Osteoarthritis Cartilage.* **2014**, *22*, 578.
14. Combe, R.; Bramwell, S.; Field, M.J. *Neurosci. Lett.* **2004**, *370*, 236.
15. Goodman's The Pharmacological Basis of Therapeutics; Hardman, L. G., Limbird, L. E., Eds., 10th ed.; McGraw-Hill: New York, 2001. Appendix Table A-II-1.

16. Hegen, M.; Keith, J.C.; Collins, M.; Nickerson-Nutter, C.L. *Ann Rheum Dis* **2008**, *67*, 1505.
17. Dunetz, J.R.; Xiang, Y.; Baldwin, A.; Ringling, J. *Org Lett.* **2011**, *13*, 5048.

ACCEPTED MANUSCRIPT